



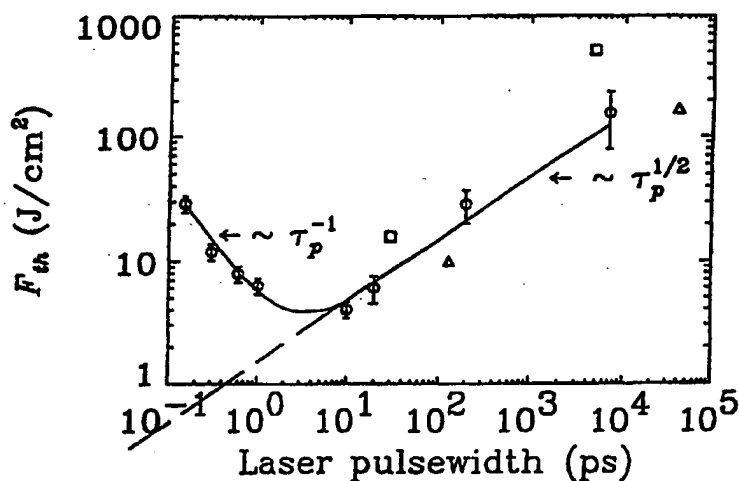
## INTERNATIONAL APPLICATION PUBLISHED UNDER THE PATENT COOPERATION TREATY (PCT)

(51) International Patent Classification <sup>6</sup> : <b>B23K 26/00, A61B 17/22</b>		A1	(11) International Publication Number: <b>WO 95/27587</b>
		(43) International Publication Date: 19 October 1995 (19.10.95)	
(21) International Application Number: PCT/US95/03863		(US). KURTZ, Ron [US/US]; Apartment No. 201, 1430 N. Dearborn, Chicago, IL 60612 (US). LICHTER, Paul [US/US]; 1100 Wolverhampton, Ann Arbor, MI 48105 (US). LIU, Xinbing [CN/US]; Apartment No. 169, 2113 Lakeview Drive, Ypsilanti, MI 48198 (US). PRONKO, Peter, P. [US/US]; 7857 Baker Heights Court, Dexter, MI 48130 (US). SQUIER, Jeffrey, A. [US/US]; 1535 Covington Drive, Ann Arbor, MI 48103 (US).  (74) Agents: DESCHERE, Linda, M. et al.; Barnes, Kisselle, 3500 Penobscot Building, 645 Griswold Street, Detroit, MI 48226 (US).  (81) Designated States: AM, AT, AU, BB, BG, BR, BY, CA, CH, CN, CZ, DE, DK, EE, ES, FI, GB, GE, HU, IS, JP, KE, KG, KP, KR, KZ, LK, LR, LT, LU, LV, MD, MG, MN, MW, MX, NL, NO, NZ, PL, PT, RO, RU, SD, SE, SG, SI, SK, TJ, TM, TT, UA, UG, US, UZ, VN, European patent (AT, BE, CH, DE, DK, ES, FR, GB, GR, IE, IT, LU, MC, NL, PT, SE), OAPI patent (BF, BJ, CF, CG, CI, CM, GA, GN, ML, MR, NE, SN, TD, TG), ARIPO patent (KE, MW, SD, SZ, UG).	
(22) International Filing Date: 29 March 1995 (29.03.95)			
(30) Priority Data: 08/224,961 8 April 1994 (08.04.94) US			
(60) Parent Application or Grant (63) Related by Continuation US 08/224,961 (CON) Filed on 8 April 1994 (08.04.94)			
(71) Applicant (for all designated States except US): THE REGENTS OF THE UNIVERSITY OF MICHIGAN [US/US]; Technology Management Office, The University of Michigan, Wolverine Tower, Room 2071, 3003 S. State Street, Ann Arbor, MI 48109-1280 (US).			
(72) Inventors; and (75) Inventors/Applicants (for US only): MOUROU, Gérard, A. [FR/US]; 4151 Thornoaks Drive, Ann Arbor, MI 48104 (US). DU, Detao [CN/US]; 2385 Bishop #7, Ann Arbor, MI 48105 (US). DUTTA, Subrata, K. [US/US]; 1608 White Street #3, Ann Arbor, MI 48104 (US). ELNER, Victor [US/US]; 1495 Morehead Drive, Ann Arbor, MI 48103			

Published

With international search report.

(54) Title: METHOD FOR CONTROLLING CONFIGURATION OF LASER INDUCED BREAKDOWN AND ABLATION



## (57) Abstract

In one aspect the invention provides a method for laser induced breakdown of a material with a pulsed laser beam where the material is characterized by a relationship of fluence breakdown threshold ( $F_{th}$ ) versus laser beam pulse width ( $T$ ) that exhibits an abrupt, rapid, and distinct change or at least a clearly detectable and distinct change in slope at a predetermined laser pulse width value. The method comprises generating a beam of laser pulses in which each pulse has a pulse width equal to or less than the predetermined laser pulse width value. The beam is focused to a point at or beneath the surface of a material where laser induced breakdown is desired. The beam may be used in combination with a mask in the beam path. The beam or mask may be moved in the X, Y and Z directions to produce desired features. The technique can produce features smaller than the spot size and Rayleigh range due to enhanced damage threshold accuracy in the short pulse regime.

**FOR THE PURPOSES OF INFORMATION ONLY**

Codes used to identify States party to the PCT on the front pages of pamphlets publishing international applications under the PCT.

AT	Austria	GB	United Kingdom	MR	Mauritania
AU	Australia	GE	Georgia	MW	Malawi
BB	Barbados	GN	Guinea	NE	Niger
BE	Belgium	GR	Greece	NL	Netherlands
BF	Burkina Faso	HU	Hungary	NO	Norway
BG	Bulgaria	IE	Ireland	NZ	New Zealand
BJ	Benin	IT	Italy	PL	Poland
BR	Brazil	JP	Japan	PT	Portugal
BY	Belarus	KE	Kenya	RO	Romania
CA	Canada	KG	Kyrgyzstan	RU	Russian Federation
CF	Central African Republic	KP	Democratic People's Republic of Korea	SD	Sudan
CG	Congo	KR	Republic of Korea	SE	Sweden
CH	Switzerland	KZ	Kazakhstan	SI	Slovenia
CI	Côte d'Ivoire	LI	Liechtenstein	SK	Slovakia
CM	Cameroon	LK	Sri Lanka	SN	Senegal
CN	China	LU	Luxembourg	TD	Chad
CS	Czechoslovakia	LV	Latvia	TG	Togo
CZ	Czech Republic	MC	Monaco	TJ	Tajikistan
DE	Germany	MD	Republic of Moldova	TT	Trinidad and Tobago
DK	Denmark	MG	Madagascar	UA	Ukraine
ES	Spain	ML	Mali	US	United States of America
FI	Finland	MN	Mongolia	UZ	Uzbekistan
FR	France			VN	Viet Nam
GA	Gabon				

METHOD FOR CONTROLLING CONFIGURATION  
OF LASER INDUCED BREAKDOWN AND ABLATION

5

Government Rights

This invention was made with government support provided by the Office of Naval Research and the National Science Foundation under the terms of No. STC PHY  
10 8920108. The government has certain rights in the invention.

Field of the Invention

This invention relates generally to methods  
15 utilizing lasers for modifying internal and external surfaces of material such as by ablation or changing properties in structure of materials. This invention may be used for a variety of materials.

20 Background of the Invention

Laser induced breakdown of a material causes chemical and physical changes, chemical and physical breakdown, disintegration, ablation, and vaporization. Lasers provide good control for procedures which require  
25 precision such as inscribing a micro pattern. Pulsed rather than continuous beams are more effective for many procedures, including medical procedures. A pulsed laser beam comprises bursts or pulses of light which are of very short duration, for example, on the order of 10  
30 nanoseconds in duration or less. Typically, these pulses

are separated by periods of quiescence. The peak power of each pulse is relatively high often on the order of  
5 gigawatts and capable of intensity on the order of  $10^{13}$  w/cm<sup>2</sup>. Although the laser beam is focused onto an area having a selected diameter, the effect of the beam extends beyond the focused area or spot to adversely affect peripheral areas adjacent to the spot. Sometimes  
10 the peripheral area affected is several times greater than the spot itself. This presents a problem, particularly where tissue is affected in a medical procedure. In the field of laser machining, current lasers using nanosecond pulses cannot produce features  
15 with a high degree of precision and control, particularly when nonabsorptive wavelengths are used.

It is a general object to provide a method to localize laser induced breakdown. Another object is to provide a method to induce breakdown in a preselected  
20 pattern in a material or on a material.

#### Summary of the Invention

In one aspect the invention provides a method for laser induced breakdown of a material with a pulsed  
25 laser beam where the material is characterized by a relationship of fluence breakdown threshold ( $F_{\text{th}}$ ) versus laser beam pulse width (T) that exhibits an abrupt, rapid, and distinct change or at least a clearly detectable and distinct change in slope at a  
30 predetermined laser pulse width value. The method

comprises generating a beam of laser pulses in which each pulse has a pulse width equal to or less than the  
5 predetermined laser pulse width value. The beam is focused to a point at or beneath the surface of a material where laser induced breakdown is desired.

In one aspect, the invention may be understood by further defining the predetermined laser pulse width  
10 as follows: the relationship between fluence breakdown threshold and laser pulse defines a curve having a first portion spanning a range of relatively long (high) pulse width where fluence breakdown threshold ( $F_{th}$ ) varies with the square root of pulse width ( $T^h$ ). The curve has a  
15 second portion spanning a range of short (low) pulse width relative to the first portion. The proportionality between fluence breakdown threshold and pulse width differ in the first and second portions of the curve and the predetermined pulse width is that point along the  
20 curve between its first and second portions. In other words, the predetermined pulse width is the point where the  $F_{th}$  versus  $\tau_p$  relationship no longer applies, and, of course, it does not apply for pulse widths shorter than the predetermined pulse width.

25 The scaling of fluence breakdown threshold ( $F_{th}$ ) as a function of pulse width ( $T$ ) is expressed as  $F_{th}$  proportional to the square root of ( $T^h$ ) is demonstrated in the pulse width regime to the nanosecond range. The invention provides methods for operating in pulse widths  
30 to the picosecond and femtosecond regime where we have

found that the breakdown threshold ( $F_{th}$ ) does not vary with the square root of pulse width ( $T_{\frac{1}{2}}$ ).

5           Pulse width duration from nanosecond down to the femtosecond range is accomplished by generating a short optical pulse having a predetermined duration from an optical oscillator. Next the short optical pulse is stretched in time by a factor of between about 500 and  
10   10,000 to produce a timed stretched optical pulse to be amplified. Then, the time stretched optical pulse is amplified in a solid state amplifying media. This includes combining the time stretched optical pulse with an optical pulse generated by a second laser used to pump  
15   the solid state amplifying media. The amplified pulse is then recompressed back to its original pulse duration.

          In one embodiment, a laser oscillator generates a very short pulse on the order of 10 to 100 femtoseconds at a relatively low energy, on the order of 0.001 to 10  
20   nanjoules. Then, it is stretched to approximately 100 picoseconds to 1 nanosecond and 0.001 to 10 nanjoules. Then, it is amplified to typically on the order of 0.001 to 1,000 millijoules and 100 picoseconds to 1 nanosecond and then recompressed. In its final state it is 10 to  
25   200 femtoseconds and 0.001 to 1,000 millijoules. Although the system for generating the pulse may vary, it is preferred that the laser medium be sapphire which includes a titanium impurity responsible for the lasing action.

In one aspect, the method of the invention provides a laser beam which defines a spot that has a lateral gaussian profile characterized in that fluence at or near the center of the beam spot is greater than the threshold fluence whereby the laser induced breakdown is ablation of an area within the spot. The maximum intensity is at the very center of the beam waist. The beam waist is the point in the beam where wave-front becomes a perfect plane; that is, its radius of curvature is infinite. This center is at radius  $R = 0$  in the x-y axis and along the Z axis,  $Z = 0$ . This makes it possible to damage material in a very small volume  $Z = 0$ ,  $R = 0$ . Thus it is possible to make features smaller than spot size in the x-y focal plane and smaller than the Rayleigh range (depth of focus) in the Z axis. It is preferred that the pulse width duration be in the femtosecond range although pulse duration of higher value may be used so long as the value is less than the pulse width defined by an abrupt or discernable change in slope of fluence breakdown threshold versus laser beam pulse width.

In another aspect, a diaphragm, disk, or mask is placed in the path of the beam to block at least a portion of the beam to cause the beam to assume a desired geometric configuration. In still further aspects, desired beam configurations are achieved by varying beam spot size or through Fourier Transform (FT) pulse shaping to cause a special frequency distribution to provide a geometric shape.

It is preferred that the beam have an energy in the range of 10 nJ (nanojoules) to 1 millijoule and that the beam have a fluence in the range of 0.1 J/cm<sup>2</sup> to 100 J/cm<sup>2</sup> (joules per centimeter square). It is preferred that the wavelength be in a range of 200 nm (nanometers) to 1  $\mu$ m (micron).

Advantageously, the invention provides a new method for determining the optimum pulse width duration regime for a specific material and a procedure for using such regime to produce a precisely configured cut or void in or on a material. For a given material the regime is reproducible by the method of the invention. Advantageously, very high intensity results from the method with a modest amount of energy and the spot size can be very small. Damage to adjoining area is minimized which is particularly important to human and animal tissue.

These and other object features and advantages of the invention will be become apparent from the following description of the preferred embodiments, claims, and accompanying drawings.

#### Brief Description of the Drawings

Figure 1 is a schematic representation of a laser induced breakdown experimental system which includes a chirped pulse amplification laser system and means for detecting scattered and transmitted energy. If the sample is transparent, then transmitted energy can also be measured.



Figure 2 is a plot of scattered energy versus incident fluence obtained for an opaque (gold) sample using the system in Figure 1 operated at 150 femtoseconds (fs) pulse duration.

Figure 3 is a plot of calculated and experimental values of threshold fluence versus pulse width for gold, with experimental values obtained for the gold sample using the system of Figure 1 operated at 800 nm wavelength. The arrow shows the point on the plot where the  $F_{th}$  proportional to  $T^4$  no longer applies, as this relationship only holds for pulse widths down to a certain level as shown by the solid line.

Figure 4 is a graphical representation of sub-spot size ablation/machining in gold based on arbitrary units and showing  $F_{th}$  the threshold fluence needed to initiate material removal;  $R_s$  the spot size of the incident beam and  $R_a$  the radius of the ablated hole in the x-y plane.

Figure 5 is a schematic illustration of a beam intensity profile showing that for laser micro-machining with ultrafast pulse according to the invention, only the peak of the beam intensity profile exceeds the threshold intensity for ablation/machining.

Figure 6A and B are schematic illustrations of a beam showing the placement of a disk-shaped mask in the beam path.

Figure 7 is a plot of scattered plasma emission and transmitted laser pulse as a function of incident laser pulse energy for a transparent glass sample,  $\text{SiO}_2$ .

Figure 8 is a plot of fluence threshold ( $F_{th}$ ) versus pulse width (T) for the transparent glass sample of Figure 7 showing that  $F_{th}$  varying with  $T^h$  only holds for pulse widths down to a certain level as shown by the solid line. Previous work of others is shown in the long pulse width regime (Squares, Smith Optical Eng 17, 1978 and Triangles, Stokowski, NBS Spec Bul 541, 1978).

Figure 9 is a plot of fluence threshold versus pulse width for corneal tissue, damage threshold for cornea, again showing that the proportionality between  $F_{th}$  and pulse width follows the  $T^h$  relationship only for pulse widths which are relatively long.

Figures 10 and 11 are plots of plasma emission versus laser fluence showing that at 170fs (Figure 10) pulse width the  $F_{th}$  is very clearly defined compared to 7ns (Figure 11) pulse width where it is very unclear. Figures 10 and 11 both show breakdown data for human cornea at, respectively, 170fs and 7ns.

Figure 12 is a plot of impact ionization rate per unit distance determined by experiment and theoretical calculation.

Figures 13A and B are schematic illustrations of beam profile along the longitudinal Z axis and showing precise control of damage - dimension along the Z axis.

### Detailed Description of the Preferred Embodiments

Referring to Figure 1 there is shown an apparatus for performing tests to determine the laser induced breakdown threshold as a function of laser pulse width in the nanosecond to femtosecond range using a chirped-pulse amplification (CPA) laser system. The basic configuration of such a CPA system is described in U.S. Patent No. 5,235,606 which is assigned to the assignee of the present invention and which has inventors in common with this present application. U.S. Patent No. 5,235,606 is incorporated herein by reference in its entirety.

Chirped-pulse amplification systems have been described by Jeffrey Squier and Gerard Mourou, two of the joint inventors in the present application, in a publication entitled Laser Focus World published by Pennwell in June of 1992. It is described that CPA systems can be roughly divided into four categories. The first includes the high energy low repetition systems such as ND glass lasers with outputs of several joules but they may fire less than 1 shot per minute. A second category are lasers that have an output of approximately 1 joule and repetition rates from 1 to 20 hertz. The third group consists of millijoule level lasers that operate at rates ranging from 1 to 10 kilohertz. A fourth group of lasers operates at 250 to 350 kilohertz and produces a 1 to 2 microjoules per pulse. In 5,235,606 several solid state amplifying materials are identified and the invention of 5,235,606 is illustrated

5 using the Alexandrite. The examples below use Ti:Sapphire and generally follow the basic process of 5,235,606 with some variations as described below.

10 The illustrative examples described below generally pertain to pulse energies less than a microjoule and often in the nanojoule range with pulse duration in the range of hundreds of picoseconds or less and the frequency on the order of 1 kilohertz. But these examples are merely illustrative and the invention is not limited thereby.

15 In a basic scheme for CPA, first a short pulse is generated. Ideally the pulse from the oscillator is sufficiently short so that further pulse compression is not necessary. After the pulse is produced it is stretched by a grating pair arranged to provide positive group velocity dispersion. The amount the pulse is stretched depends on the amount of amplification. Below 20 a millijoule, tens of picoseconds are usually sufficient. A first stage of amplification typically takes place in either a regenerative or a multipass amplifier. In one configuration this consists of an optical resonator that contains the gain media, a Pockels cell, and a thin film polarizer. After the regenerative amplification stage 25 the pulse can either be recompressed or further amplified. The compressor consists of a grating or grating pair arranged to provide negative group velocity dispersion. Gratings are used in the compressor to correspond to those in the stretching stage. More 30

particulars of a typical system are described in U.S. Patent No. 5,235,606, previously incorporated herein by reference.

5       An important aspect of the invention is the development of a characteristic curve of fluence breakdown threshold  $F_{th}$  as a function of laser pulse width specific to a material. Then identify on such curve, the point at which there is an abrupt, or distinct and rapid change or at least a discernable change in  
10       slope characteristic of the material. In general it is more desirable to operate past this point because of the more precise control of the laser induced breakdown (LIB) or ablation threshold.

15       Example 1 - Opaque Material

Figure 1 shows an experimental setup for determining threshold fluence by determining scattered energy versus incident fluence and by determining threshold fluence versus pulse width. The system  
20       includes means for generating a pulsed laser beam as described earlier, and means, typically a lens, for collecting emission from the target to a photomultiplier tube. Change of transmission through a transparent sample is measured with an energy meter.

25       Figure 2 shows a plot of data obtained from an absorbing medium which is gold using 150 fs pulse and Figure 3 shows threshold fluence versus pulse width. The arrow in Figure 3 identifies the point at which the relationship between the threshold fluence and pulse  
30       width varies dramatically.

In experimental conditions with wavelength of 800 nm and 200 fs pulses on gold (Figure 3), the absorption depth is 275 Å with a diffusion length of 50 Å. In the case of nanosecond pulses the diffusion length, which is on the order of 10 μm (micron) in diameter, is much longer than the absorption depth, resulting in thermal diffusion being the limiting factor in feature size resolution. Empirical evidence for the existence of these two regimes is as exhibited in Figure 3. Here both experimental and theoretical ablation thresholds are plotted as a function of pulse width. An arrow at approximately 7 picoseconds pulse width (designated herein as  $T$  or  $\tau_p$ ) delineates the point (or region closely bounding that point) at which the thermal diffusion length ( $l_{th}$ ) is equal to the absorption depth ( $1/a$ ). It is clear that for a smaller size spot a shorter (smaller) pulse is necessary. For spot size on the order of 1000 Å or less, pulse width on the order of 100 femtoseconds or less will be needed. It is clear from the figure that this is the point at which the ablation threshold transitions from a slowly varying or nearly constant value as a function of pulse width to one that is dramatically dependent on pulse time. This result is surprising. It has been demonstrated that the electron thermalization time for laser deposited energy in gold is on the order of, or less than, 500 fs and the electron-lattice interaction time is 1 ps. The consequences of this for ultrafast laser pulses is that

the energy is contained within the beam spot. In fact for energies at or near the threshold for ablation, the spatial profile of the laser beam will determine the size and shape of the region being ablated (Figures 4 and 5).

Additional experiments were performed to measure the amount of recombination light produced as a function of the fluence impinging on a gold film. The technique involved is based upon the experimental setup previously described. A basic assumption is that the intensity of the light is proportional to the amount of material ablated. In Figure 4, the material removed is plotted as a function of fluence. A well defined threshold fluence is observed at which material removal is initiated. By having only a small fraction of the gaussian beam where the fluence is greater than the threshold, the ablated region can be restricted to this small area. In Figure 4,  $R_t$  is the radial position on the beam where the fluence is at threshold. Ablation, then, occurs only within a radius  $R_t$ . It is evident that by properly choosing the incident fluence, the ablated spot or hole can in principle be smaller than the spot size,  $R_t$ . This concept is shown schematically in Figure 5. Although the data for a 150 fs pulse is shown in Figure 4, this threshold behavior is exhibited in a wide range of pulse widths. However, sub spot size ablation is not possible in the longer pulse regimes, due to the dominance of thermal diffusion as will be described below.

Additional experiments on opaque materials used  
a 800 nm Ti:Sapphire oscillator whose pulses were  
5 stretched by a grating pair, amplified in a regenerative  
amplifier operating at 1 kHz, and finally recompressed by  
another grating pair. Pulse widths from 7 ns to 100 fs  
were obtained. The beam was focused with a 10x objective,  
implying a theoretical spot size of 3.0  $\mu\text{m}$  in diameter. A  
10 SEM photo-micrograph of ablated holes obtained in a  
silver film on glass, using a pulse width of 200 fs and a  
pulse energy of 30 nJ (fluence of 0.4 J/cm<sup>2</sup>) produced two  
holes of diameter approximately 0.3  $\mu\text{m}$  in diameter.  
Similar results have been obtained in aluminum.

15 These results suggest that by, producing a  
smaller spot size which is a function of numerical  
aperture and wavelength, even smaller holes can be  
machined. We have demonstrated the ability to generate  
the fourth harmonic (200 nm) using a nonlinear crystal.  
20 Thus by using a stronger objective lens along with the  
200 nm light, holes with diameters of 200 angstroms could  
in principle be formed.

These examples show that by using femtosecond  
pulses the spatial resolution of the ablation/machining  
25 process can be considerably less than the wavelength of  
the laser radiation used to produce it. The ablated  
holes have an area or diameter less than the area or  
diameter of the spot size. In the special case of  
diffraction limited spot size, the ablated hole has a  
30 size (diameter) less than the fundamental wavelength



size. We have produced laser ablated holes with diameters less than the spot diameter and with diameters 10% or less of the laser beam spot size. For ultrafast pulses  
5 in metals the thermal diffusion length,  $l_{th} = (Dt)^{1/2}$  (where D is the thermal diffusivity and t the pulse time), is significantly smaller than the absorption depth  $(1/a)$ , where a is the absorption coefficient for the radiation.

Those skilled in the art will understand that  
10 the basic method of the invention may be utilized in alternative embodiments depending on the desired configurations of the induced breakdown. Examples include, but are not limited to using a mask in the beam path, varying spot size, adjusting focus position by  
15 moving the lens, adjusting laser cavity design, Fourier Transform (FT) shaping, using a laser operating mode other than TEM<sub>00</sub>, and adjusting the Rayleigh range, the depth of focus or beam waist.

The use of a mask is illustrated in Figure 6A  
20 and B. The basic method consists of placing a mask in the beam path or on the target itself. If it is desired to block a portion of the beam, the mask should be made of an opaque material and be suspended in the beam path (Figure 6A) alternatively, the mask may be placed on the  
25 target and be absorptive so as to contour the target to the shape of the mask (Figure 6B).

The varying spot size is accomplished by  
varying the laser f/#, i.e., varying the focal length of the lens or input beam size to the lens as by adjustable  
30 diaphragm.

Operation in other than the TEM<sub>00</sub> mode means that higher order transverse modes could be used. This affects the beam and material as follows: the beam need not be circular or gaussian in intensity. The material will be ablated corresponding to the beam shape.

The Rayleigh range (Z axis) may be adjusted by varying the beam diameter, where the focal plane is in the x-y axis.

#### Example 2 - Transparent Material

A series of tests were performed on an SiO<sub>2</sub> (glass) sample to determine the laser induced breakdown (LIB) threshold as a function of laser pulse width between 150 fs - 7 ns, using a CPA laser system. The short pulse laser used was a 10 Hz Ti:Sapphire oscillator amplifier system based on the CPA technique. The laser pulse was focused by an f = 25 cm lens inside the SiO<sub>2</sub> sample. The Rayleigh length of the focused beam is ~ 2 mm. The focused spot size was measured in-situ by a microscope objective lens. The measured spot size FWHM (full width at half max) was 26 μm in diameter in a gaussian mode. The fused silica samples were made from Corning 7940, with a thickness of 0.15 mm. They were optically polished on both sides with a scratch/dig of 20-10. Each sample was cleaned by methanol before the experiment. Thin samples were used in order to avoid the complications of self-focusing of the laser pulses in the bulk. The SiO<sub>2</sub> sample was mounted on a computer

controlled motorized X-Y translation stage. Each  
location on the sample was illuminated by the laser only  
5 once.

Two diagnostics were used to determine the  
breakdown threshold  $F_{th}$ . First, the plasma emission from  
the focal region was collected by a lens to a  
photomultiplier tube with appropriate filters. Second,  
10 the change of transmission through the sample was  
measured with an energy meter. (See Figure 1) Visual  
inspection was performed to confirm the breakdown at a  
nanosecond pulse duration. Figure 7 shows typical plasma  
emission and transmitted light signal versus incident  
15 laser energy plots, at a laser pulse width of  $\tau_p = 300$   
fs. It is worth noting that the transmission changed  
slowly at around  $F_{th}$ . This can be explained by the  
temporal and spatial behavior of the breakdown with  
ultrashort pulses. Due to the spatial variation of the  
20 intensity, the breakdown will reach threshold at the  
center of the focus, and because of the short pulse  
duration, the generated plasma will stay localized. The  
decrease in transmitted light is due to the reflection,  
scattering, and absorption by the plasma. By assuming a  
25 gaussian profile in both time and space for the laser  
intensity, and further assuming that the avalanche takes  
the entire pulse duration to reach threshold, one can  
show that the transmitted laser energy  $U_t$  as a function  
of the input energy  $U$  is given by

$$U_t = kU,$$

$$U \leq U_{th}$$

$$U_t = kU_{th}[1 + \ln(U/U_{th})], \quad U > U_{th}$$

5

where  $k$  is the linear transmission coefficient. The solid curve in Figure 7 is plotted using Eq. (1), with  $U_{th}$  as a fitting parameter. In contrast, breakdown caused by nanosecond laser pulses cuts off the transmitted beam near the peak of the pulses, indicating a different temporal and spatial behavior.

Figure 8 shows the fluence breakdown threshold  $F_{th}$  as a function of laser pulse width. From 7 ns to about 10 ps, the breakdown threshold follows the scaling in the relatively long pulse width regime (triangles and squares) are also shown as a comparison - it can be seen that the present data is consistent with earlier work only in the higher pulse width portion of the curve. When the pulse width becomes shorter than a few picoseconds, the threshold starts to increase. As noted earlier with respect to opaque material (metal), this increased precision at shorter pulse widths is surprising. A large increase in damage threshold accuracy is observed, consistent with the multiphoton avalanche breakdown theory. (See Figures 8 and 9.) It is possible to make features smaller than spot size in the x-y focal plane and smaller than the Rayleigh range (depth of focus) in the longitudinal direction or Z axis. These elements are essential to making features smaller than spot size or Rayleigh range.

Example 3 - Tissue

A series of experiments was performed to determine the breakdown threshold of cornea as a function of laser pulse width between 150 fs - 7 ns, using a CPA laser system. As noted earlier, in this CPA laser system, laser pulse width can be varied while all other experimental parameters (spot size, wavelength, energy, etc.) remain unchanged. The laser was focused to a spot size (FWHM) of 26  $\mu\text{m}$  in diameter. The plasma emission was recorded as a function of pulse energy in order to determine the tissue damage threshold. Histologic damage was also assessed.

Breakdown thresholds calculated from plasma emission data revealed deviations from the scaling law,  $F_{th} \propto T^4$ , as in the case of metals and glass. As shown in Figure 9, the scaling law of the fluence threshold is true to about 10 ps, and fails when the pulse shortens to less than a few picoseconds. As shown in Figures 10 and 11, the ablation or LIB threshold varies dramatically at high (long) pulse width. It is very precise at short pulse width. These results were obtained at 770 nm wavelengths. The standard deviation of breakdown threshold measurements decreased markedly with shorter pulses. Analysis also revealed less adjacent histological damage with pulses less than 10 ps.

The breakdown threshold for ultrashort pulses (< 10 ps) is less than longer pulses and has smaller standard deviations. Reduced adjacent histological damage to tissue results from the ultrashort laser pulses.

In summary, it has been demonstrated that sub-wavelength holes can be machined into metal surfaces using femtosecond laser pulses. The effect is physically understood in terms of the thermal diffusion length, over the time period of the pulse deposition, being less than the absorption depth of the incident radiation. The interpretation is further based on the hole diameter being determined by the lateral gaussian distribution of the pulse in relation to the threshold for vaporization and ablation.

Laser induced optical breakdown dielectrics consists of three general steps: free electron generation and multiplication, plasma heating and material deformation or breakdown. Avalanche ionization and multiphoton ionization are the two processes responsible for the breakdown. The laser induced breakdown threshold in dielectric material depends on the pulse width of the laser pulses. An empirical scaling law of the fluence breakdown threshold as a function of the pulse width is given by  $F_{th} \propto \sqrt{\tau_p}$ , or alternatively, the intensity breakdown threshold,  $I_{th} = F_{th}/\tau_p$ . Although this scaling law applies in the pulse width regime from nanosecond to tens of picoseconds, the invention takes advantage of the heretofore unknown regime where breakdown threshold does not follow the scaling law when suitably short laser pulses are used, such as shorter than 7 picoseconds for gold and 10 picoseconds for  $\text{SiO}_2$ .

While not wishing to be held to any particular theory, it is thought that the ionization process of a solid dielectric illuminated by an intense laser pulse can be described by the general equation

$$\frac{dn_e(t)}{dt} = \eta(E)n_e(t) + \left(\frac{dn_e(t)}{dt}\right)_{pi} - \left(\frac{dn_e(t)}{dt}\right)_{loss}$$

where  $n_e(t)$  is the free electron (plasma) density,  $\eta(E)$  is the avalanche coefficient, and  $E$  is the electric field strength. The second term on the right hand side is the photoionization contribution, and the third term is the loss due to electron diffusion, recombination, etc. When the pulse width is in the picosecond regime, the loss of the electron is negligible during the duration of the short pulse.

Photoionization contribution can be estimated by the tunneling rate. For short pulses,  $E \sim 10^8$  V/cm, the tunneling rate is estimated to be  $w \sim 4 \times 10^9$  sec<sup>-1</sup>, which is small compared to that of avalanche, which is derived below. However, photoionization can provide the initial electrons needed for the avalanche processes at short pulse widths. For example, the data shows at 1 ps, the rms field threshold is about  $5 \times 10^7$  V/cm. The field will reach a value of  $3.5 \times 10^7$  V/cm (rms) at 0.5 ps before the peak of the pulse, and  $w \sim 100$  sec<sup>-1</sup>. During a  $\Delta t \sim 100$  fs period the electron density can reach  $n_e \sim n_v[1 - \exp(-w\Delta t)] \sim 10^{11}$  cm<sup>-3</sup>, where  $n_v \sim 10^{22}$  is the total initial valence band electron density.

Neglecting the last two terms there is the case of an electron avalanche process, with impact ionization by primary electrons driven by the laser field. The electron density is then given by  $n_e(t) = n_0 \times \exp(n(E)t)$ , where  $n_0$  is the initial free electron density. These initial electrons may be generated through thermal ionization of shallow traps or photoionization. When assisted by photoionization at short pulse regime, the breakdown is more statistical. According to the condition that breakdown occurs when the electron density exceeds  $n_{th} \approx 10^{18} \text{ cm}^{-3}$  and an initial density of  $n_0 \approx 10^{10} \text{ cm}^{-3}$ , the breakdown condition is then given by  $\eta\tau_e \approx 18$ . For the experiment, it is more appropriate to use  $n_{th} \approx 1.6 \times 10^{21} \text{ cm}^{-3}$ , the plasma critical density, hence the threshold is reached when  $\eta\tau_e \approx 30$ . There is some arbitrariness in the definition of plasma density relating to the breakdown threshold. However, the particular choice of plasma density does not change the dependence of threshold as function of pulse duration (the scaling law).

In the experiment, the applied electric field is on the order of a few tens of MV/cm and higher. Under such a high field, the electrons have an average energy of  $\sim 5 \text{ eV}$ , and the electron collision time  $\tau$  is less than  $0.4 \text{ fs}$  for electrons with energy  $U \geq 5 - 6 \text{ eV}$ . Electrons will make more than one collision during one period of the electric oscillation. Hence the electric field is essentially a dc field to those high energy electrons.



The breakdown field at optical frequencies has been shown to correspond to dc breakdown field by the relationship  $E_{\text{th}}^{\text{opt}}(w) = E_{\text{th}}^{\text{dc}}(1 + w^2\tau^2)^{1/2}$ , where  $w$  is the optical frequency and  $\tau$  is the collision time.

In dc breakdown, the ionization rate per unit length,  $\alpha$ , is used to describe the avalanche process, with  $\eta = \alpha(E)v_{\text{drift}}$ , where  $v_{\text{drift}}$  is the drift velocity of electrons. When the electric field is as high as a few MV/cm, the drift velocity of free electrons is saturated and independent of the laser electric field,  $v_{\text{drift}} \approx 2 \times 10^7$  cm/s.

The ionization rate per unit length of an electron is just  $eE/U_1$  times the probability,  $P(E)$ , that the electron has an energy  $\geq U_1$ , or  $\alpha(E) = (eE/U_1)P(E)$ . Denoting  $E_{\text{KT},2p}$ , and  $E_1$  as threshold fields for electrons to overcome the decelerating effects of thermal, phonon, and ionization scattering, respectively. Then the electric field is negligible,  $E < E_{\text{KT}}$ , so the distribution is essentially thermal,  $P(E)$  is simply  $\exp(-U_1/kT)$ . It has been suggested:  $P(E) \sim \exp(-\text{const}/E)$  for  $E_{\text{KT}} < E < E_p$ ;  $P(E) \sim \exp(-\text{const}/E^2)$  at higher fields ( $E > E_p$ ). Combining the three cases the expression that satisfies both low and high field limits:

$$\alpha(E) = (eE/U_1) \exp(-E_1/(E(1+E/E_p)+E_{\text{KT}})).$$

This leads to  $F_{\text{th}} \propto E^2\tau_p \sim 1/\tau_p$ , i.e., the fluence threshold will increase for ultrashort laser pulses when  $E > \sqrt{E_p E_1}$  is satisfied.

Figure 12 is a plot of  $\alpha$  as a function of the electric field,  $E$ . From experimental data, calculated  $\alpha$  according to  $\eta r_p = 30$  and  $\eta = av_{drift}$ . The solid curve is calculated from the above equation, using  $E_i = 30$  MV/cm,  $E_p = 3.2$  MV/cm, and  $E_{kt} = 0.01$  MV/cm. These parameters are calculated from  $U = eEl$ , where  $U$  is the appropriate thermal, phonon, and ionization energy, and  $l$  is the correspondent energy relation length ( $l_{kt} = l_p \sim 5$  Å, the atomic spacing, and  $l_i \sim 30$  Å). It shows the same saturation as the experimental data. The dashed line is corrected by a factor of 1.7, which results in an excellent fit with the experimental data. This factor of 1.7 is of relatively minor importance, as it can be due to a systematic correction, or because breakdown occurred on the surface first, which could have a lower threshold. The uncertainty of the saturation value of  $v_{drift}$  also can be a factor. The most important aspect is that the shape (slope) of the curve given by the equation provides excellent agreement with the experimental data. Thus, the mechanism of laser induced breakdown in fused silica (Example 2), using pulses as short as 150 fs and wavelength at 780 nm, is likely still dominated by the avalanche process.

Opaque and transparent materials have common characteristics in the curves of Figures 3, 8, and 9 each begins with  $F_{th}$  versus  $T^1$  behavior but then distinct change from that behavior is evident. From the point of deviation, each curve is not necessarily the same since

the materials differ. The physical characteristics of  
5 each material differ requiring a material specific  
analysis. In the case of  $\text{SiO}_2$  (Figure 8) the energy  
deposition mechanism is by dielectric breakdown. The  
optical radiation is releasing electrons by multiphoton  
10 ionization (M PI) that are tightly bound and then  
accelerating them to higher energies by high field of two  
lasers. It is thought that only a small amount of  
relatively high energy electrons exist prior to the laser  
action. The electrons in turn collide with other bound  
15 electrons and release them in the avalanching process. In  
the case of metal, free electrons are available and  
instantly absorbing and redistributing energy. For any  
material, as the pulses get shorter, laser induced  
breakdown (LIB) or ablation occurs only in the area where  
20 the laser intensity exceeds LIB or ablation threshold.  
There is essentially insufficient time for the  
surrounding area to react thermally. As pulses get  
shorter, vapor from the ablated material comes off after  
the deposition of the pulse, rather than during  
25 deposition, because the pulse duration is so short. It  
was also observed that the laser intensity also varies  
along the propagation axis (Figure 13). The beam  
intensity as a function of R and Z expressed as:

30 
$$I(Z, R) = I_0 / (1 + Z/Z_R)^2 \cdot \exp(-2R^2/W^2_z)$$

5 where  $Z_R$  is the Rayleigh range and is equal to  $Z_R = \frac{\pi W_0^2}{\lambda}$ .  
 $W_0$  is the beam size at the waist ( $Z = 0$ ).

We can see that the highest value of the field is at  $Z = R = 0$  at the center of the waist. If the threshold is precisely defined it is possible to damage the material precisely at the waist and have a damaged volume representing only a fraction of the waist in the R direction or in the Z direction. It is very important to control precisely the damage threshold or the laser intensity fluctuation.

15 For example, if the damage threshold or the laser fluctuation is known within 10% that means that on the axis ( $R = 0$ )

20 
$$I(0,Z)/I_0 = 1/(1 + (Z/Z_R)^2) = .9$$

damaged volume can be produced at a distance  $Z_R/3$  where  $Z_R$  again is the Rayleigh range. For a beam waist of  $W_0 = \lambda$  then  $Z_R = \frac{\pi W_0^2}{\lambda} = \pi \lambda$  and the distance between hole can be  $Z_R \frac{\pi \lambda}{3}$  as shown in Figure 13.

25 The maximum intensity is exactly at the center of the beam waist ( $Z = 0, R = 0$ ). For a sharp threshold it is possible to damage transparent, dielectric material

30

in a small volume centered around the origin point ( $Z = 0$ ,  $R = 0$ ). The damage would be much smaller than the beam waist in the  $R$  direction. Small cavities, holes, or damage can have dimensions smaller than the Rayleigh range ( $Z_R$ ) in the volume of the transparent, dielectric material. In another variation, the lens can be moved to increase the size of the hole or cavity in the  $Z$  dimension. In this case, the focal point is essentially moved along the  $Z$  axis to increase the longitudinal dimension of the hole or cavity. These features are important to the applications described above and to related applications such as micro machining, integrated circuit manufacture, and encoding data in data storage media.

Advantageously, the invention identifies the regime where breakdown threshold fluence does not follow the scaling law and makes use of such regime to provide greater precision of laser induced breakdown, and to induce breakdown in a preselected pattern in a material or on a material. The invention makes it possible to operate the laser where the breakdown or ablation threshold becomes essentially accurate. The accuracy can be clearly seen by the I-bars along the curves of Figures 8 and 9. The I-bars consistently show lesser deviation and correspondingly greater accuracy in the regime at or below the predetermined pulse width.

While this invention has been described in terms of certain embodiment thereof, it is not intended that it be limited to the above description, but rather only to the extent set forth in the following claims.

The embodiments of the invention in which an  
exclusive property or privilege is claimed are defined in  
5 the appended claims.

We Claim:

1.

- 5 A method for laser induced breakdown (LIB) of a material with a pulsed laser beam, the material being characterized by a relationship of fluence breakdown threshold versus laser pulse width that exhibits a rapid and distinct change in slope at a predetermined laser pulse width, said method comprising the steps of:
- 10 a. generating a beam of one or more laser pulses in which each pulse has a pulse width equal to or less than said predetermined laser pulse width; and
- 15 b. focusing said beam to a point at or beneath the surface of the material.

2.

- The method according to claim 1 wherein the material is metal, the pulse width is 10 to 10,000 femtoseconds, and the beam has an energy of 1 nanojoule to 1 microjoule.
- 20

3.

- The method according to claim 1 wherein the laser beam defines a spot and has a lateral gaussian profile characterized in that fluence at or near the center of the beam spot is greater than the threshold fluence whereby the laser induced breakdown is ablation of an area within the spot.
- 25

4.

The method according to claim 3 wherein the spot size is a diffraction limited spot size providing an ablation cavity having a diameter less than the  
5 fundamental wavelength size.

5.

The method according to claim 1 wherein the material is transparent to laser wavelength and the pulse  
10 width is 10 to 10,000 femtoseconds, the beam has an energy of 10 nanojoules to 1 millijoule.

6.

The method according to claim 1 wherein the  
15 material is biological tissue, the pulse width is 10 to 10,000 femtoseconds and the beam has an energy of 10 nanojoules to 1 millijoule.

7.

The method according to claim 1 wherein the  
20 predetermined pulse width is obtained by measuring the ablation (LIB) threshold of the material as a function of pulse width and determining where the ablation (LIB) threshold function no longer scales as the square root of  
25 pulse width.

8.

The method according to claim 1 wherein the  
30 laser beam has an energy in a range of 10 nanojoules to 1 millijoule.



9.

The method according to claim 1 wherein the laser beam has a fluence in a range of 100 millijoules per square centimeter to 100 joules per square  
5 centimeter.

10.

The method according to claim 1 wherein the laser beam defines a spot in or on the material and the LIB causes ablation of an area having a size smaller than  
10 the area of the spot.

11.

The method according to claim 1 wherein the laser beam has a wavelength in a range of 200 nanometers to 2 microns.  
15

12.

The method according to claim 1 wherein the pulse width is in a range of a few picoseconds to femtoseconds.  
20

13.

The method according to claim 1 wherein the breakdown includes chemical and physical changes.  
25

14.

The method according to claim 1 wherein the breakdown includes chemical and physical breakdown.

15.

The method according to claim 1 wherein the breakdown includes disintegration.

5

16.

The method according to claim 1 wherein the breakdown includes ablation.

10

17.

The method according to claim 1 wherein the breakdown includes vaporization.

15

18.

The method according to claim 1 wherein the spot size is varied by flexible diaphragm to a range of 1 to 100 microns.

20

19.

The method according to claim 1 wherein a mask is placed in the path of the beam to block a portion of the beam to cause the beam to assume a desired geometric configuration.

25

20.

The method according to claim 1 wherein the laser operating mode is non-TEM<sub>00</sub>.

30

21.

A method for laser induced breakdown of a material which comprises:

- 5                   a.     generating a beam of one or more laser pulses comprising a sequence of pulses in which each pulse has a pulse width equal to or less than a pulse width value corresponding to a change in slope of a curve of fluence breakdown threshold ( $F_{th}$ ) as a function of laser pulse width ( $T$ ), said change occurring at a point between
- 10                   first and second portions of said curve, said first portion spanning a range of relatively long pulse width where  $F_{th}$  varies with the square root of pulse width ( $T^{1/2}$ ) and said second portion spanning a
- 15                   range of short pulse width relative to said first portion with a  $F_{th}$  versus  $T$  slope which differs from that of said first portion; and
- 20                   b.     focusing said beam to a point at or beneath the surface of the material.

## 22.

The method according to claim 21 and further including:

- 25                   a.     identifying a pulse width start point;
- b.     focussing the laser beam initial start point at or beneath the surface of the material; and
- 30                   c.     scanning said beam along a predetermined path in a transverse direction.

23.

5       The method according to claim 21 and further  
including:

- a.     identifying a pulse width start point;
- b.     focussing the laser beam initial start  
point at or beneath the surface of the  
material; and
- 10    c.     scanning said beam along a predetermined  
path in a longitudinal direction in the  
material to a depth smaller than the  
Rayleigh range.

15

24.

The method according to claim 21 wherein the  
breakdown includes chemical and physical changes.

25.

20

The method according to claim 21 wherein the  
breakdown includes chemical and physical breakdown.

26.

25       The method according to claim 21 wherein the  
breakdown includes disintegration.

27.

The method according to claim 21 wherein the  
breakdown includes ablation.

28.

5     The method according to claim 21 wherein the  
breakdown includes vaporization.

29.

A method for laser induced breakdown of a  
material which comprises:

- 10     a.     determining, for a selected material, a  
characteristic curve of fluence breakdown  
threshold ( $F_{th}$ ) as a function of laser  
pulse width;
- 15     b.     identifying a pulse width value on said  
curve corresponding to a rapid and  
distinct change in slope of said  $F_{th}$   
versus pulse width curve characteristic of  
said material;
- 20     c.     generating a beam of one or more laser  
pulses, said beam comprising a sequence of  
pulses having a pulse width at or below  
said pulse width value corresponding to  
said distinct change in slope; and
- 25     d.     focusing said beam to a point at or  
beneath the surface of the material.

30.

The method according to claim 29 and further  
including:

- 30     a.     identifying a pulse width start point;

- 5
- b. focussing the laser beam initial start point at or beneath the surface of the material; and
  - c. scanning said beam along a predetermined path in a transverse direction.

## 31.

The method according to claim 29 and further including:

- 10
- a. identifying a pulse width start point;
  - b. focussing the laser beam initial start point at or beneath the surface of the material; and
  - 15 c. scanning said beam along a predetermined path in a longitudinal direction in the material to a depth smaller than the Rayleigh range.

## 32.

20 The method according to claim 29 wherein the breakdown includes chemical and physical changes.

## 33.

25 The method according to claim 29 wherein the breakdown includes chemical and physical breakdown.

## 34.

The method according to claim 29 wherein the breakdown includes disintegration.

35.

The method according to claim 29 wherein the breakdown includes ablation.

5

36.

The method according to claim 29 wherein the breakdown includes vaporization.

37.

10

The method according to any one of claims 1, 2, 5, 6, 21, and 29 wherein said beam is obtained by chirped-pulse amplification (CPA) means comprising means for generating a short optical pulse having a predetermined duration; means for stretching such optical pulse in time; means for amplifying such time-stretched optical pulse including solid state amplifying media; and means for recompressing such amplified pulse to desired duration.

15

20

38.

The method according to claim 1 wherein the spot size is varied within a range of 1 to 100 microns by changing the f number of the laser beam.

25

39.

The method according to claim 1 wherein the spot size is varied within a range of 1 to 100 microns by varying the target position.

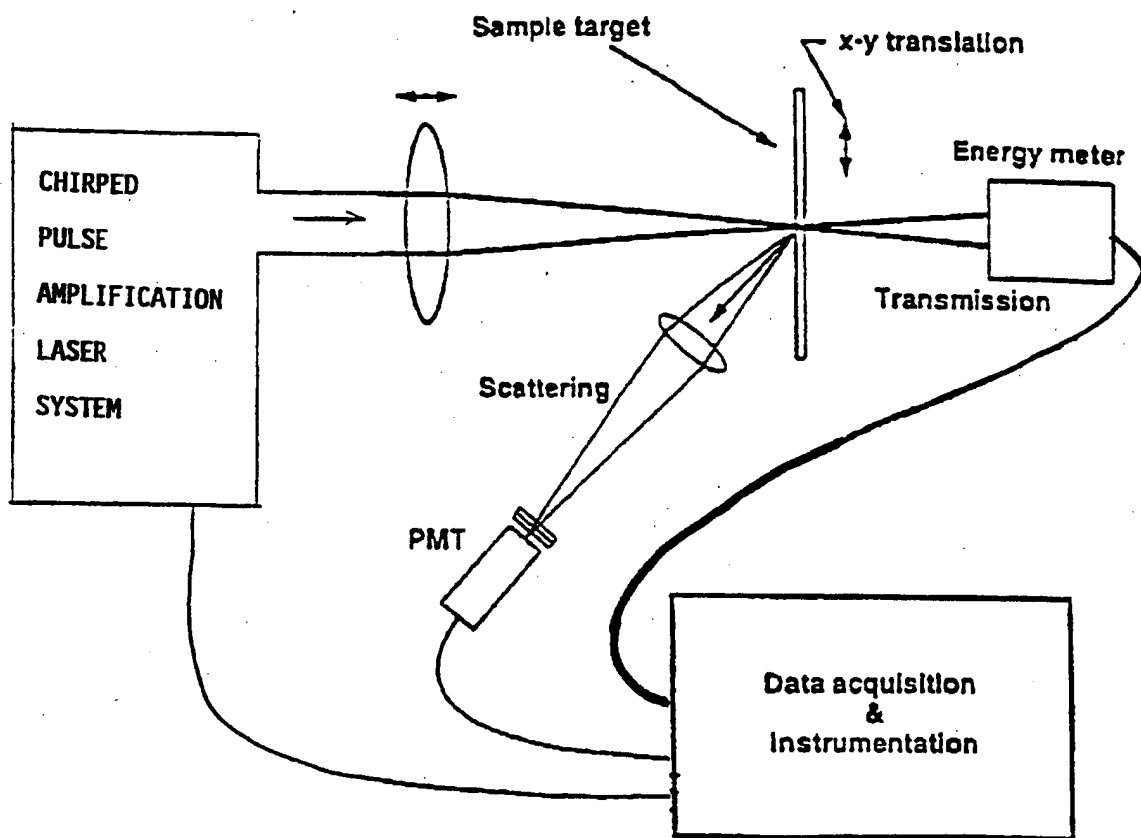


FIGURE 1



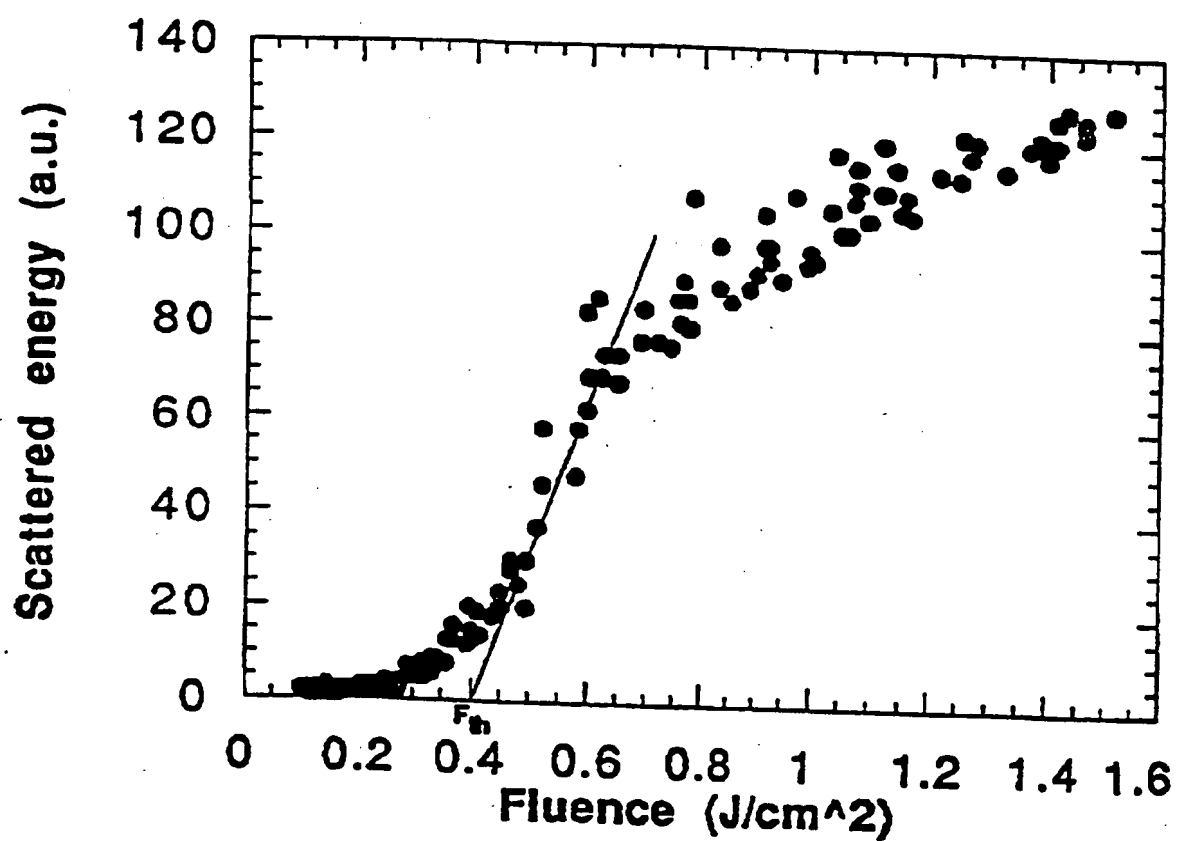


FIGURE 2

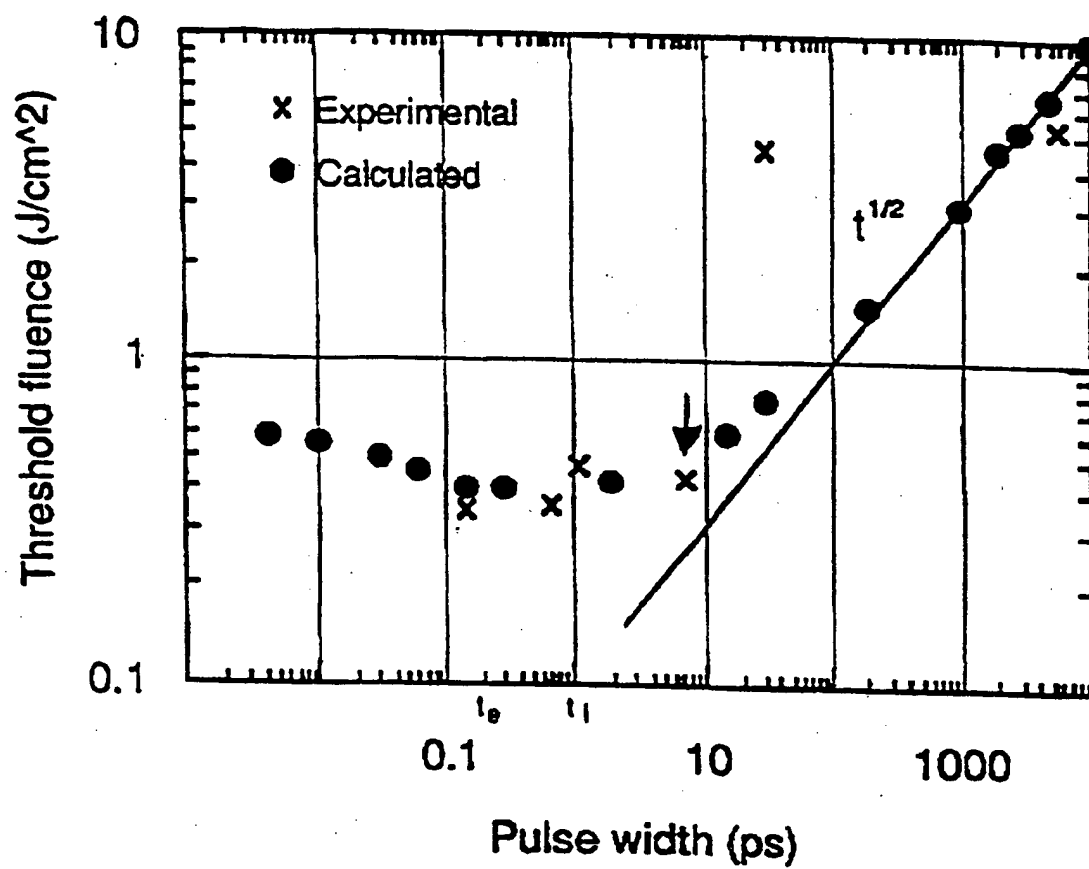


FIGURE 3

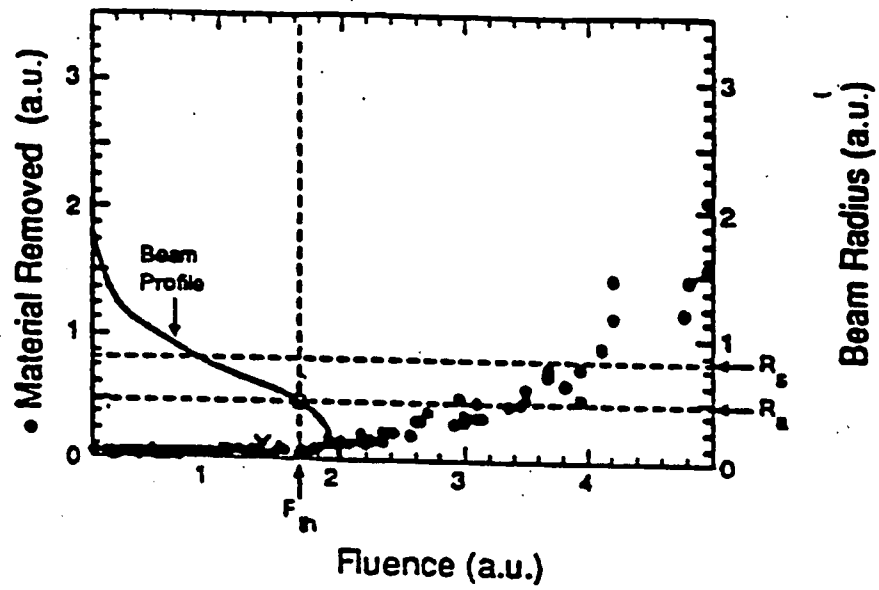


FIGURE 4

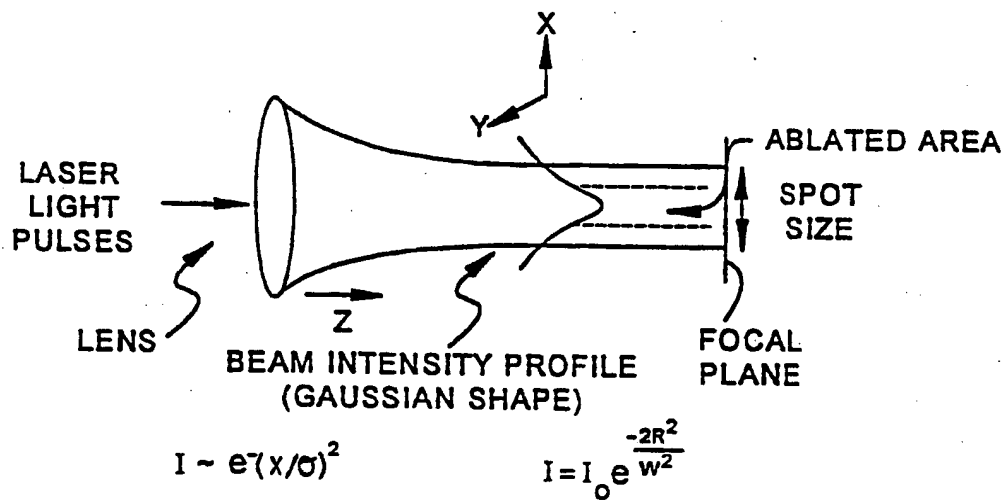
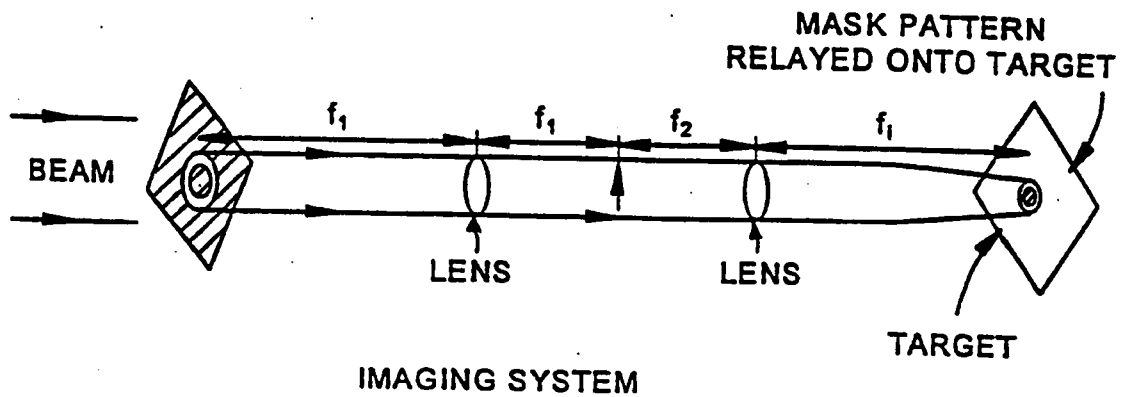


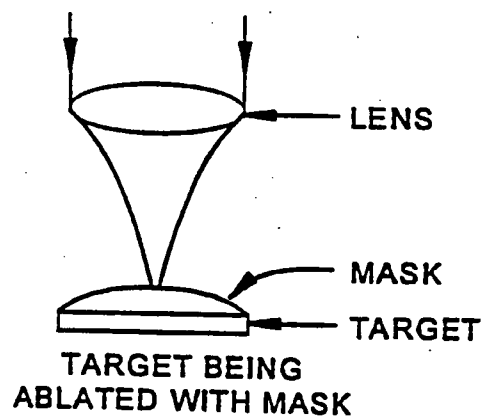
FIG.5

$f_1, f_2$  - FOCAL LENGTH OF LENSES  
 $f_1 = mf_2$  WHERE  $m$  IS ARBITRARY



MASK - CROSS HATCHED AREAS  
 ARE OPAQUE TO LASER WAVELENGTH

FIG.6A



TARGET AFTER ABLATION IS ESSENTIALLY  
 IMAGE OF MASK.

TARGET AFTER ABLATION

FIG.6B

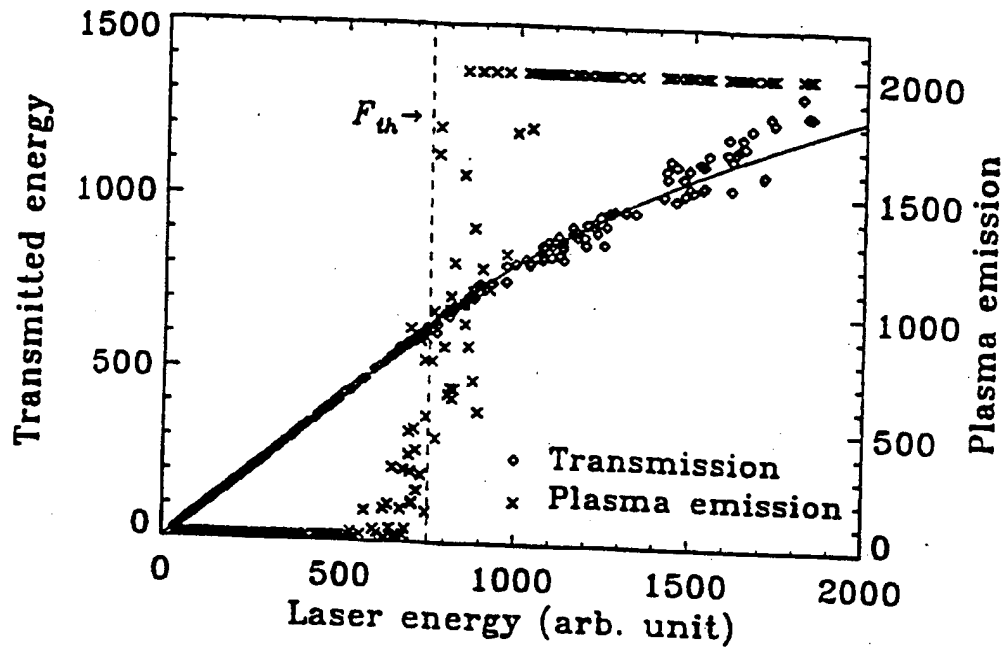


FIGURE 7

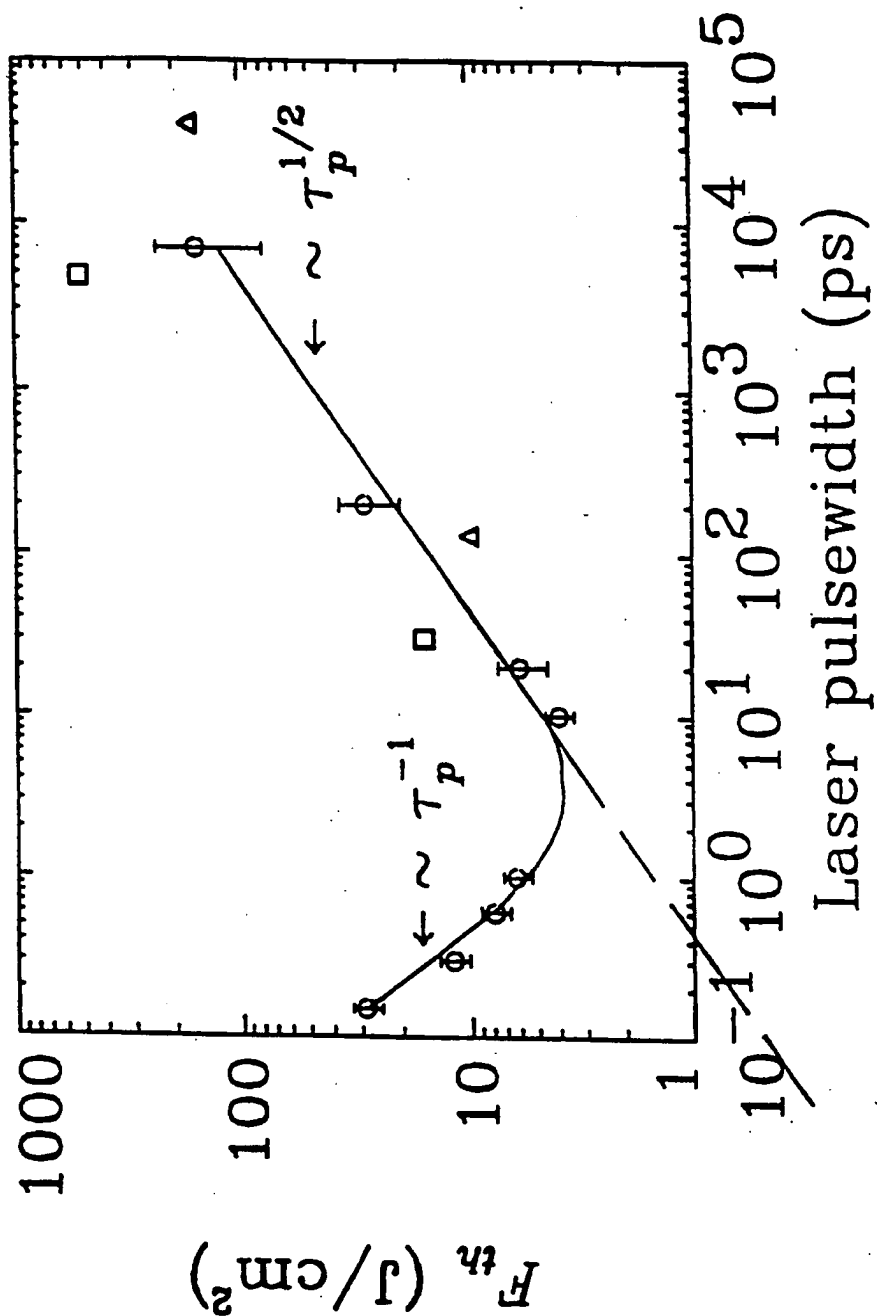


FIGURE 8

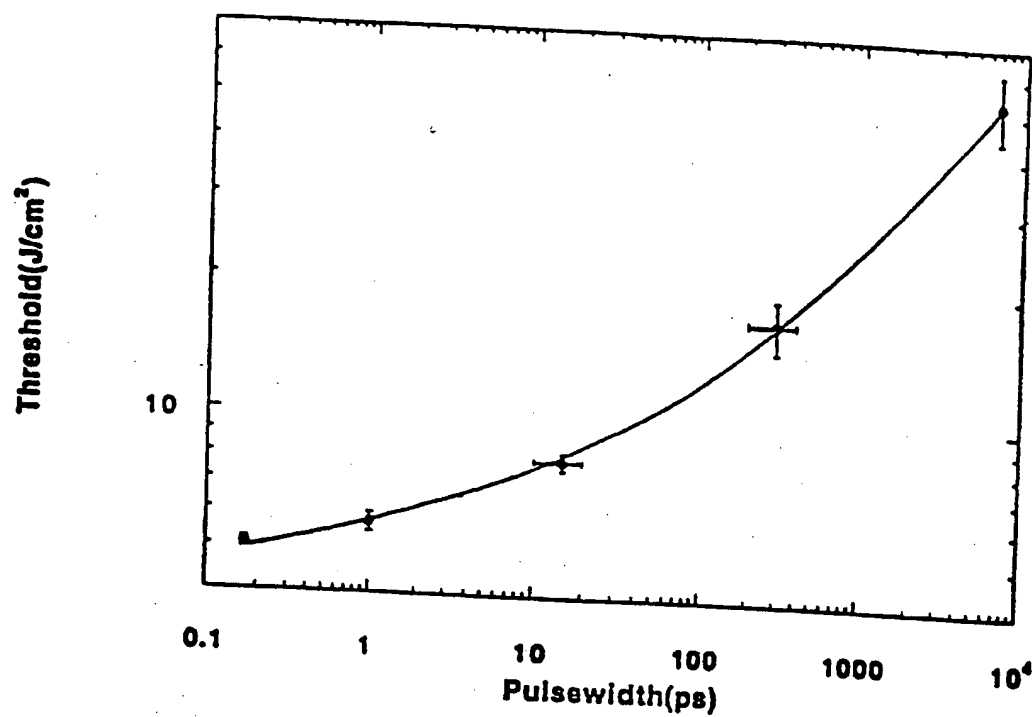


FIGURE 9

9/13

SUBSTITUTE SHEET (RULE 26)



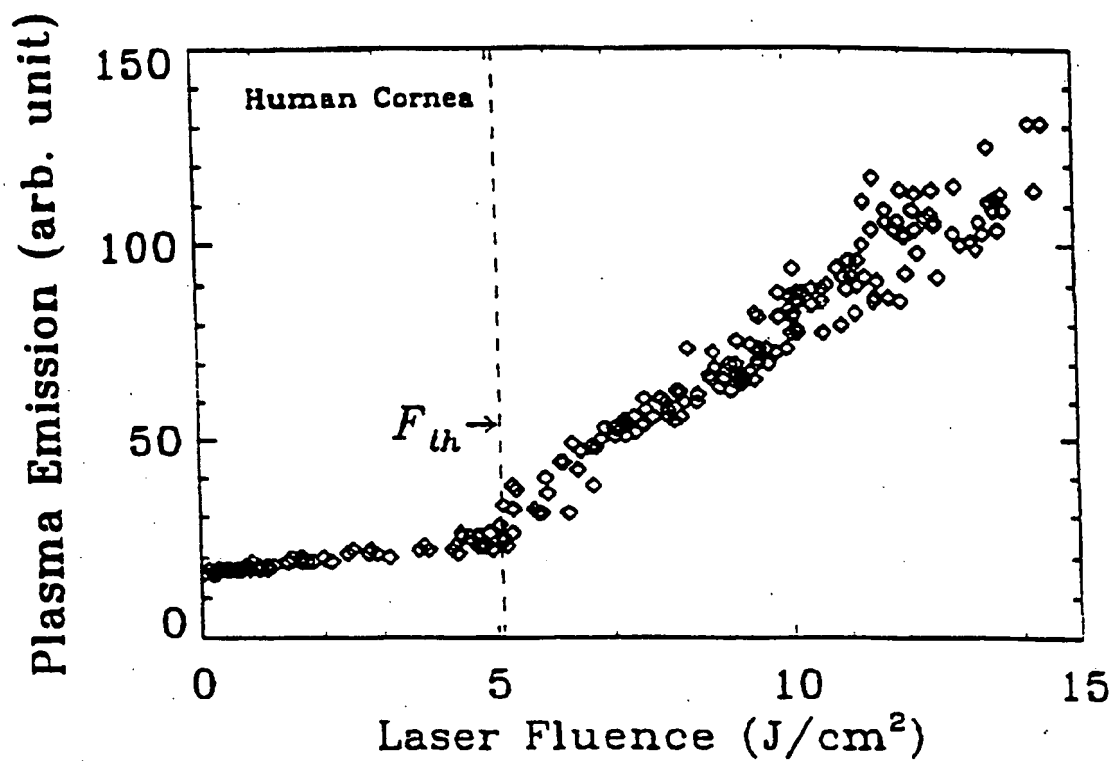


FIGURE 10

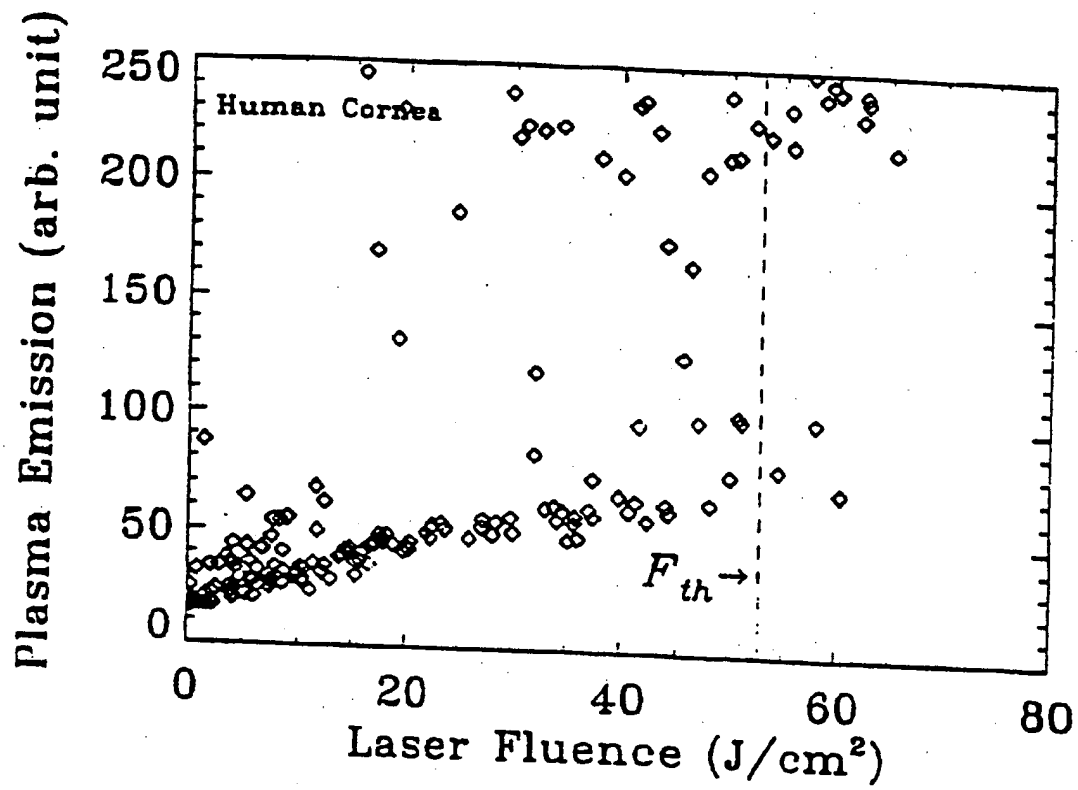


FIGURE 11

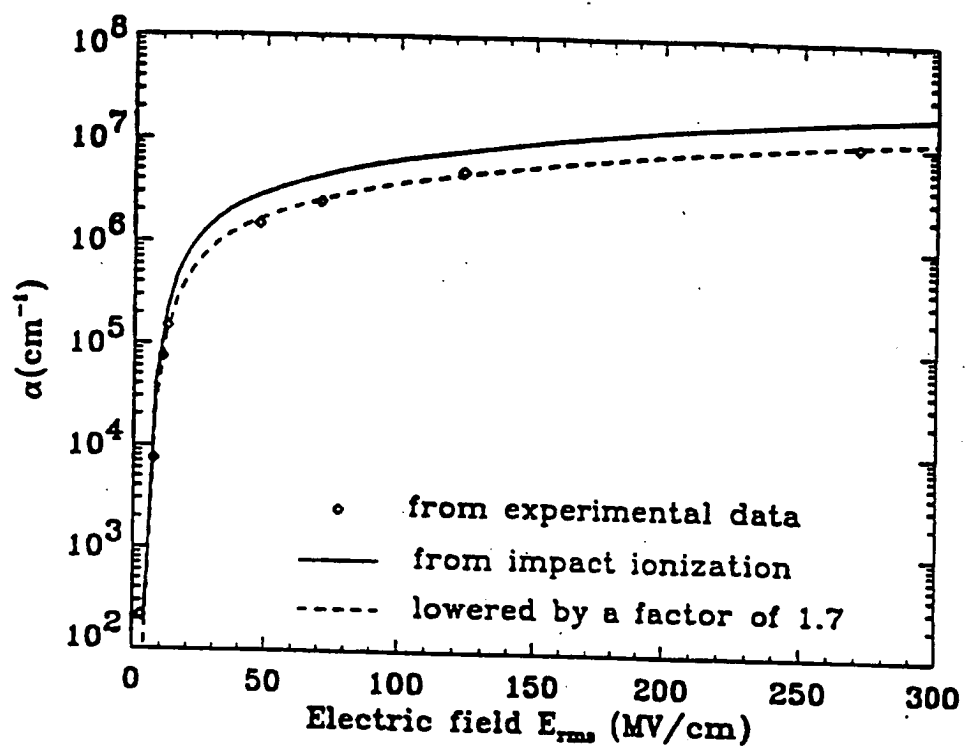


FIGURE 12

DAMAGE ALONG THE Z AXIS

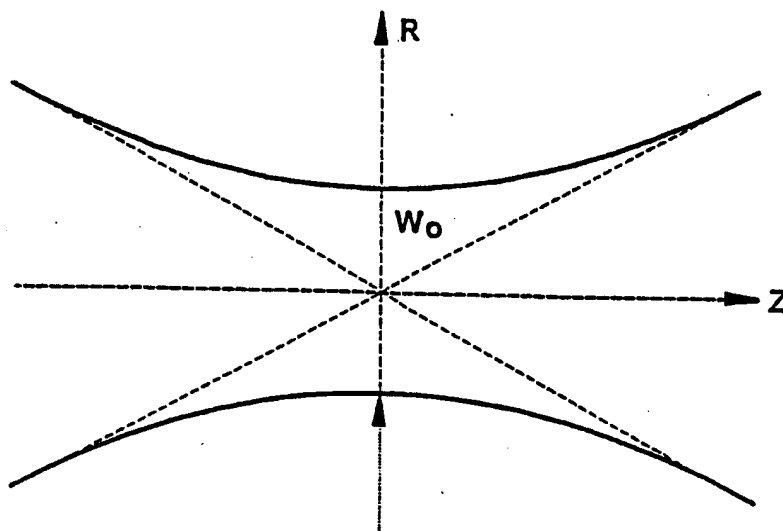


FIG. 13A

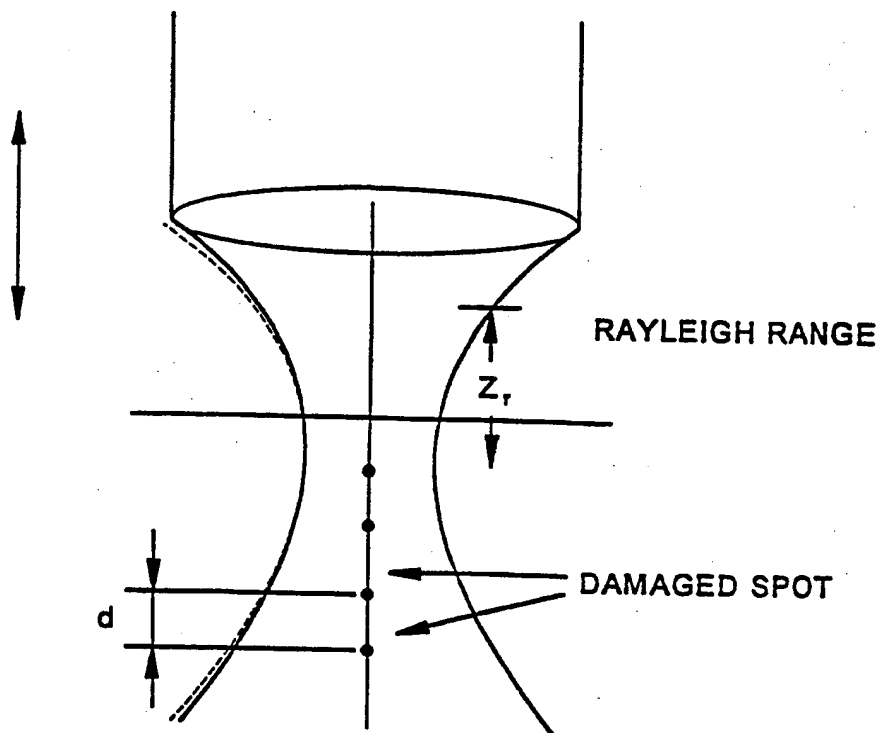


FIG. 13B

# INTERNATIONAL SEARCH REPORT

International Application No  
PCT/US 95/03863

A. CLASSIFICATION OF SUBJECT MATTER  
IPC 6 B23K26/00 A61B17/22

According to International Patent Classification (IPC) or to both national classification and IPC

## B. FIELDS SEARCHED

Minimum documentation searched (classification system followed by classification symbols)  
IPC 6 B23K A61B

Documentation searched other than minimum documentation to the extent that such documents are included in the fields searched

Electronic data base consulted during the international search (name of data base and, where practical, search terms used)

## C. DOCUMENTS CONSIDERED TO BE RELEVANT

Category *	Citation of document, with indication, where appropriate, of the relevant passages	Relevant to claim No.
A	SCIENCE, vol. 213, no. 31, July 1981 LANCASTER ( USA ), pages 505-512, BERNS ET AL. 'Laser microsurgery in cell and developmental biology' summary ---	1,2,5,6, 11-13,21
A	DE,A,41 19 024 (TECHNOLAS LASER TECHNIK GMBH) 17 December 1992 see the whole document ---- -/--	1,21-23

☒ Further documents are listed in the continuation of box C.

☒ Patent family members are listed in annex.

### \* Special categories of cited documents :

- \* "A" document defining the general state of the art which is not considered to be of particular relevance
- \* "E" earlier document but published on or after the international filing date
- \* "L" document which may throw doubts on priority claim(s) or which is cited to establish the publication date of another citation or other special reason (as specified)
- \* "O" document referring to an oral disclosure, use, exhibition or other means
- \* "P" document published prior to the international filing date but later than the priority date claimed

- \* "T" later document published after the international filing date or priority date and not in conflict with the application but cited to understand the principle or theory underlying the invention
- \* "X" document of particular relevance; the claimed invention cannot be considered novel or cannot be considered to involve an inventive step when the document is taken alone
- \* "Y" document of particular relevance; the claimed invention cannot be considered to involve an inventive step when the document is combined with one or more other such documents, such combination being obvious to a person skilled in the art.
- \* "&" document member of the same patent family

Date of the actual completion of the international search

31 July 1995

Date of mailing of the international search report

- 4. 08. 95

Name and mailing address of the ISA

European Patent Office, P.B. 5818 Patentlaan 2  
NL - 2280 HV Rijswijk  
Tel. ( + 31-70 ) 340-2040, Tx. 31 651 epo nl,  
Fax ( + 31-70 ) 340-3016

Authorized officer

Herbreteau, D

# INTERNATIONAL SEARCH REPORT

Int. Application No  
PCT/US 95/03863

## C(Continuation) DOCUMENTS CONSIDERED TO BE RELEVANT

Category *	Citation of document, with indication, where appropriate, of the relevant passages	Relevant to claim No.
A	<p>IEEE TRANSACTIONS ON BIOMEDICAL ENGINEERING, vol. 40, no. 2, February 1993 NEW-YORK (USA), pages 188-200, XP 000380289 LE CARPENTIER ET AL. 'Continuous wave laser ablation of tissue: analysis of thermal and mechanical events' see the whole document ----</p>	1-39
A	<p>ANN. PHYS., vol. 19, no. 1, February 1994 FRANCE, LE BLANC 'Realization and characterization of a high intensity femtosecond laser system based on all titatium doped sapphire' Abstract -----</p>	1,2,5

### Information on patent family members

**PCT/US 95/03863**

Form PCT/ISA/210 (patent family annex) (July 1992)

**THIS PAGE BLANK (USPTO)**



**This Page is Inserted by IFW Indexing and Scanning  
Operations and is not part of the Official Record**

**BEST AVAILABLE IMAGES**

Defective images within this document are accurate representations of the original documents submitted by the applicant.

Defects in the images include but are not limited to the items checked:

- ☐ **BLACK BORDERS**
- ☐ **IMAGE CUT OFF AT TOP, BOTTOM OR SIDES**
- ☒ **FADED TEXT OR DRAWING**
- ☐ **BLURRED OR ILLEGIBLE TEXT OR DRAWING**
- ☐ **SKEWED/SLANTED IMAGES**
- ☐ **COLOR OR BLACK AND WHITE PHOTOGRAPHS**
- ☐ **GRAY SCALE DOCUMENTS**
- ☒ **LINES OR MARKS ON ORIGINAL DOCUMENT**
- ☐ **REFERENCE(S) OR EXHIBIT(S) SUBMITTED ARE POOR QUALITY**
- ☐ **OTHER:** \_\_\_\_\_

**IMAGES ARE BEST AVAILABLE COPY.**

**As rescanning these documents will not correct the image problems checked, please do not report these problems to the IFW Image Problem Mailbox.**

**THIS PAGE BLANK (USPTO)**